Radio Science

RESEARCH ARTICLE
10.1029/2019RS006974

Special Section:
Special Issue of the 2019 URSI Asia-Pacific Radio Science Conference

FFT-Based Multiband Spectrum Sensing in SIMO In-band Full-Duplex Cognitive Radio Networks

Tripta[1], **Abhishek Kumar**[1], **and Seemanti Saha**[1]

[1]Department of Electronics and Communication Engineering, National Institute of Technology Patna, Patna, India

Key Points:
- FFT-based multiband spectrum sensing using two-dimensional averaging is proposed in full-duplex cognitive radio networks
- Related test statistic and closed form expressions for average detection and false alarm probability are obtained
- Wavelet decomposition-based least squares technique is employed for digital domain residual self-interference cancelation

Correspondence to:
A. Kumar,
abhishek.ece14@nitp.ac.in

Citation:
Tripta, Kumar, A., & Saha, S. (2020). FFT-based multiband spectrum sensing in SIMO in-band full-duplex cognitive radio networks. *Radio Science*, *55*, e2019RS006974. https://doi.org/10.1029/2019RS006974

Received 15 SEP 2019
Accepted 4 MAY 2020
Accepted article online 1 JUN 2020

Abstract This paper presents fast Fourier transform (FFT)-based multiband spectrum sensing over multipath Rayleigh frequency selective fading channels in single input multiple output (SIMO) in-band full-duplex (FD) cognitive radio (CR) networks (FDCRNs) under residual self-interference (RSI). In this work, first, multiband energy detection using Neyman Pearson criterion is proposed in FDCRNs under RSI, where the secondary user is equipped with multiple receive antennas to exploit spatial diversity. Next, a two-dimensional averaging is done to overcome spectrum leakage problem occurring due to FFT operation in orthogonal frequency division multiplexing (OFDM) system. The closed form expressions for average probability of detection and probability of false alarm are derived for SIMO FDCRNs under RSI. Further, RSI cancelation is performed employing noise robust wavelet decomposition-based least squares scheme and the corresponding simulation studies indicate that the proposed algorithm further improves the detection performance in SIMO FDCRNs.

1. Introduction

The rapid deployment of the advance wireless technologies, providing high data rate services, such as wireless computers, smart phones, and smart homes leads to scarcity of the available radio spectrum resources (Yucek & Arslan, 2009). Cognitive radio (CR) is emerging as a potential approach for the upcoming generation of wireless communication systems to utilize the unused spectral resources dynamically (Haykin, 2005). In CR networks (CRNs), the secondary user (SU)/unlicensed user can opportunistically access the unused licensed band of the primary user (PU). Recently, the Federal Communications Commission (FCC) has reported that approximately on an average only 10% spectrum between 0 and 6 GHz band is utilized at any time (Report, 2002). Eventually, the FCC suggested the opening of licensed bands for the use of unlicensed users which results in the development of CR (Wang, 2011).

The thorough literature survey reveals that the conventional CRNs employ SUs operating in half-duplex mode in which the SUs cannot perform the sensing and transmission simultaneously using the same frequency band (Axell et al., 2012). In in-band full-duplex (FD) CR (FDCR), which is an upcoming 5G technology, SUs are capable of utilizing the same channel for both sensing and transmission and thus help to enhance the spectrum efficiency (Afifi & Krunz, 2015; Badawy et al., 2016; Tripta et al., 2017). The major hindrance in the feasibility of FD communication is the large self-interference (SI) power transmitted from the antenna within the same transceiver. SI cancelation has become the key challenge for the implementation of practical FDCR system (Nguyen et al., 2014). Generally, SI cancelation is performed in three domains: passive, active analog, and active digital. Even after passive and active analog domain cancelation, there exist some SI called residual SI (RSI), which could be further suppressed by applying efficient and reliable digital domain SI cancelation algorithms (Masmoudi & Le-Ngoc, 2015).

In FDCR networks (FDCRNs), the SU operates in FD mode using the same frequency band for sensing and transmission and thus promotes enhanced spectrum efficiency (Afifi & Krunz, 2015; Liao et al., 2014). PU signal detection/spectrum sensing is the key task for CRNs, where SU identifies the spectrum holes reliably without interfering to PU (Hossain et al., 2009). Most of the reported spectrum sensing techniques are based on low complexity energy detection schemes (Tandra & Sahai, 2005). In the context of energy detection-based spectrum sensing in FDCRNs, various literature have been reported (Badawy et al., 2016; Tripta et al., 2017), though a simple energy detection is not sufficient for detecting the presence of unused PU spectrum but it gives optimal performance for independent and identically distributed (i.i.d) random samples (Tandra & Sahai, 2005). The major drawback of the basic energy detection scheme is its inherent sensitivity toward noise variance uncertainty (Tandra & Sahai, 2005). In Vilar et al. (2011), to overcome this issue, the authors exploited the spatial correlation properties of the signal received from multiple antenna.

It is also noticed that eigenvalue-based (Dikmese et al., 2013) and augraorrelation-based (Huang & Huang, 2013) energy detection techniques are robust against noise variance uncertainty but suffer from high computational complexity. In Dikmese et al. (2012), the authors promote the multichannel wideband sensing that calibrates the noise spectral density at the sensing receiver. In practical wireless systems, the communication channel is wideband rather than narrowband, which motivates us to perform spectrum sensing in orthogonal frequency division multiplexing (OFDM) systems where spectrum analysis is facilitated by energy detection scheme based on fast Fourier transform (FFT) that reduces the computational complexity. However, the FFT operation on an unknown signal leads to spectrum leakage problem (Bloomfield, 2000). In order to smoothen the FFT output, two-dimensional averaging is performed so that a more reliable decision statistic could be obtained (Dikmese et al., 2011). In this work, we preferred to use low complexity rectangular filter for averaging the samples in time and frequency dimensions. In Dikmese et al. (2012), FFT-based detection using two-dimensional averaging to smoothen the FFT output is performed in half-duplex mode considering additive white Gaussian noise (AWGN) channel model where channel gain is considered as unity. In realistic wireless communication scenario, the signal passes through the fading channels, which is addressed in this work and the detection is carried out under multipath fading environment.

In this paper, we propose an FFT-based spectrum sensing using two-dimensional rectangular filtering operation over multipath fading channel in single input multiple output (SIMO) FDCRNs under RSI. The main contributions in this paper are summarized as follows:

- First, the analysis of the proposed technique using Neyman-Pearson criterion is carried out over multipath frequency selective fading environment in SIMO FDCRN under RSI system where, the test statistic is obtained by squaring FFT output followed by two-dimensional averaging on the signal received at SU after channel filtering, analog-to-digital conversion, and serial-to-parallel conversion.
- The closed form expressions are obtained for probabilities of average detection ($\bar{P}_d$) and false alarm (P_{fa}). The simulation studies show the impact of RSI on the detection performance, which enhances due to decrease in RSI.
- Further, the suppression of RSI is achieved by employing digital domain RSI cancelation algorithm using noise robust wavelet denoising-based least squares (LS) technique under two schemes. In the first scheme, the desired signal transmitter is kept off, whereas in the second scheme, desired signal transmitter is kept on and the desired signal is considered as noise.
- Finally, the comparative detection performance approves that the proposed wavelet denoising-based LS technique under the first scheme considering desired signal transmitter off outperforms the conventional LS techniques.

The remaining sections are organized as follows: Section 2 presents the system model of FFT-based multiband spectrum sensing using Neyman Pearson criterion over multipath fading channels under RSI. In section 3.1, analysis of the proposed energy detection technique employing two-dimensional averaging operation in SIMO FDCRNs is performed. A noise robust wavelet-based LS technique for SI channel estimation and SI cancelation is presented in section 3.2. Section 4 depicts the simulation results and finally, conclusion is conveyed in section 5.

2. System Model

Figure 1 shows the architecture of SIMO FDCRN, where SU having multiple receive antennas exploiting spatial diversity is operating in FD mode; that is, it is transmitting and sensing simultaneously. The considered transmission and sensing (TS) mode is described in Figure 2. Initially, the SU operates in half-duplex mode for time slot Ts_1 to sense the availability of PU channel. If the channel is found free, SU decides to transmit for T time slot. Once it started its transmission, it continues to sense for the return of PU signal. Total sensing duration is divided into small slots each equal to Ts_i duration where, $i = 2, 3, \dots .n$. If the SU finds channel busy, it stops its transmission.

In the narrowband analysis, the binary hypotheses H_0 and H_1 representing the absence and presence of the PU signal, respectively, are as follows:

$$\begin{aligned} H_0 &: \; y_r(n) = s_{rSI}(n) + w_r(n), \\ H_1 &: \; y_r(n) = x_{rPU}(n) + s_{rSI}(n) + w_r(n). \end{aligned} \tag{1}$$

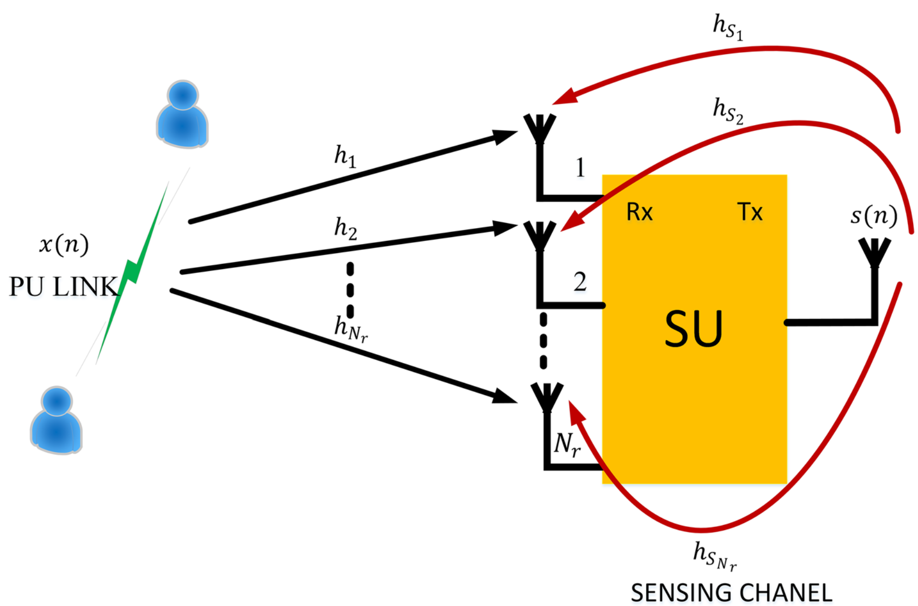

Figure 1. SIMO FDCRN sensing scenario.

Under H_0, the nth signal sample received at the rth receive antenna of SU is only noise ($w_r(n)$) with ($mean =$ 0 and $variance = \sigma^2_{w,r}$) where, n and r are given as $0 \le n \le N-1$ and $1 \le r \le N_r$, respectively, and RSI over single tap fading channel is represented as $s_{rSI}(n) = h_{sr}s(n)$ having Gaussian distribution with mean 0 and variance $\sigma^2_{S_{SI}}$. On the contrary, under H_1 we receive symbol from the desired PU transmitter as well as noise plus RSI. The PU signal received over multipath fading channel is represented as follows:

$$x_{rPU}(n) = \sum_{l=0}^{L-1} h_r(l)x(n-l), \tag{2}$$

Here, $x(n)$ is the PU transmit symbol, L represents the total number of multipath fading channel taps such that $0 \le l \le L-1$ and variance of each channel tap is represented by $\sigma^2_h(l)$.

3. Efficient Energy Detector for SIMO FDCRNs Over Frequency Selective Rayleigh Fading Channel

The block schematic diagram for the proposed FFT-based multiband spectrum sensing using two-dimensional filtering operation in FDCRNs under RSI is shown in Figure 3. Here, we consider a OFDM-based CR system with K subcarriers. The SU with multiple receive antennas is operating in FD mode, which signifies that at each receive antenna of SU, the signal from the intended PU transmitter is received along with the noise and RSI. We represent the FFT output as $Y_r[m,k]$, where m indicates the mth OFDM symbol; that is, time index and k represent the kth subcarrier of an OFDM symbol, that is, frequency index. In the present section, first, we derive the decision test static expression for performing multiple antenna energy detection in FDCRNs over frequency selective Rayleigh fading channel under RSI. Further, the detection performance of the proposed energy detection is improved employing RSI cancelation using LS technique followed by wavelet denoising for noise suppression.

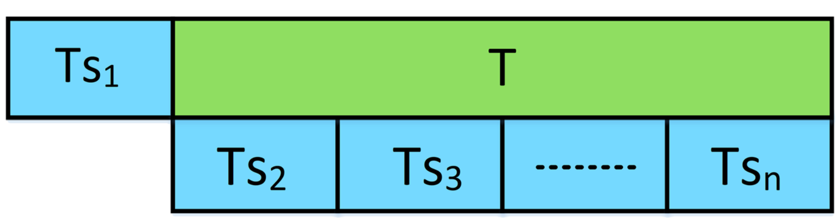

Figure 2. TS mode of operation of SU.

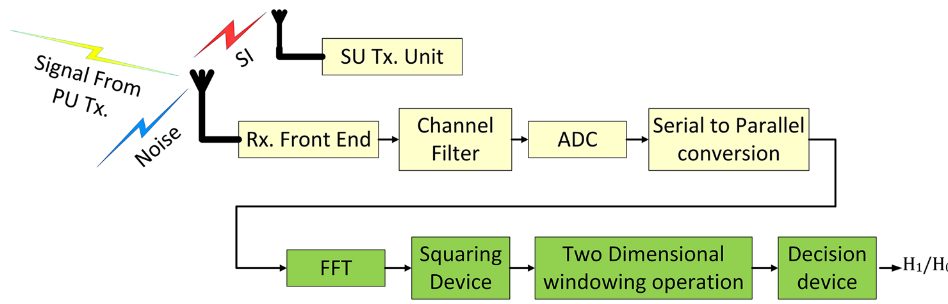

Figure 3. FFT-based energy detection using two-dimensional averaging window.

3.1. FFT-Based Multiband Energy Detection in SIMO FDCRNs Under Residual SI Over Multipath Rayleigh Frequency Selective Fading Scenario

The signal received at kth subcarrier of the mth OFDM symbol at each rth receive antenna of SU under H_0 and H_1 are expressed as follows:

$$\begin{aligned} H_0 &: \; Y_r[m,k] = S_{rSI}[m,k] + W_r[m,k], \\ H_1 &: \; Y_r[m,k] = X_{rPU}[m,k] + S_{rSI}[m,k] + W_r[m,k]. \end{aligned} \tag{3}$$

Here, $X_{rPU}[m,k]$ is the PU signal appearing at kth subcarrier of mth OFDM symbol at SU. $W_r[m,k]$ and $S_{rSI}[m,k]$ are the AWGN noise and RSI received at kth subcarrier of mth OFDM at SU and are assumed as Gaussian with $mean = 0$ and variances $\sigma^2_{W,k}$ and $\sigma^2_{S_{SI},k}$, respectively (Afifi & Krunz, 2015; Riihonen & Wichman, 2014). As multipath fading environment is considered, the signal power associated with $X_{rPU}[m,k]$ under hypothesis H_1 is considered as a random variable $X_{PU,k}$. Here, we assumed that the symbols are i.i.d, so the normalized $X_{PU,k}$ mainly depends on channel taps. To perform energy detection-based spectrum sensing, first, absolute square of the FFT output block, that is, $|Y_r[m,k]|^2$, is obtained and the test statistic using equal gain combining scheme is obtained employing filtering operation in both time and frequency domains. Now, the decision test statistic at subband level of SU is expressed as (Dikmese et al., 2012, 2015) follows:

$$T(Y[m,k]) = \frac{1}{N_r}\sum_{r=1}^{N_r}\frac{1}{N_t N_f}\sum_{k=k_0-N_f/2}^{k_0+N_f/2-1}\sum_{m=m_0-N_t+1}^{m_0}|Y_r[m,k]|^2, \tag{4}$$

where N_t and N_f are the filter lengths in time and frequency domains, respectively. m_0 and k_0 are the last position of the selected window in time and frequency domains, respectively. The test statistic is further compared with a threshold value, γ, to give the decision on the two hypotheses to be true. Mathematically, it is represented as follows:

$$T(Y[m,k]) = \frac{1}{N_r}\sum_{r=1}^{N_r}\frac{1}{N_t N_f}\sum_{k=k_0-N_f/2}^{k_0+N_f/2-1}\sum_{m=m_0-N_t+1}^{m_0}|Y_r[m,k]|^2 \geq \gamma. \tag{5}$$

As $Y_r[m,k]$ has Gaussian distribution, $T(Y[m,k])$ follows chi-square distribution. Now, if we consider $N_t.N_f$ sufficiently large approximately ≥ 10, by central limit theorem, the detector distribution follows Gaussian distribution (Arshad et al., 2010). Under hypothesis H_1, the PU signal power at kth subcarrier in mth OFDM symbol is considered as a random variable (Rodriguez-Parera et al., 2008), $X_{PU,k}$. Now, the probability density functions (PDFs) for the test statistic under both H_0 and H_1 are as follows:

$$H_0 : \; T(Y[m,k]) \sim \mathcal{N}\left(\sigma^2_{W,k} + \sigma^2_{S_{SI},k}, \frac{2}{N_r N_t N_f}(\sigma^4_{W,k} + \sigma^4_{S_{SI},k})\right) \tag{6}$$

$$H_1 : \; T(Y[m,k]) \sim \mathcal{N}\left(\sigma^2_{W,k} + \sigma^2_{S_{SI},k} + X_{PU,k}, \frac{2(\sigma^4_{W,k} + \sigma^4_{S_{SI},k} + X^2_{PU,k})}{N_r N_t N_f}\right). \tag{7}$$

Next, we derive the expression for $\bar{P_d}$ and P_{fa} using Neyman Pearson criterion that maximizes the $\bar{P_d}$ while keeping P_{fa} fixed to some constrained value. When the PU signal is absent, hypothesis H_0 is considered, which is independent of the channel, and thus, P_{fa} is defined as follows:

$$P_{fa} = P_r(T(Y[m,k]) \geq \gamma | H_0 = Q\left(\frac{\gamma - (\sigma^2_{W,k} + \sigma^2_{S_{SI},k})}{\sqrt{\frac{2(\sigma^4_{W,k}+\sigma^4_{S_{SI},k})}{N_r N_t N_f}}}\right), \tag{8}$$

$$= Q\left(\frac{\gamma - (\sigma^2_{W,k}(1+INR))}{\sigma^2_{W,k}\sqrt{\frac{2(1+INR^2)}{N_r N_t N_f}}}\right), \tag{9}$$

Here, INR is the RSI power to noise power ratio. The expression for instantaneous P_d is interpreted as follows:

$$P_d|X_{1PU,k}, X_{2PU,k}, \dots X_{N_r PU,k} = Q\left(\frac{\gamma - (\sigma^2_{W,k} + \sigma^2_{S_{SI},k} + X_{PU,k})}{\sqrt{\frac{2(\sigma^4_{W,k}+\sigma^4_{S_{SI},k}+X^2_{PU,k})}{N_r N_t N_f}}}\right). \tag{10}$$

As the detection is performed over fading channel, the P_d under H_1 is averaged over each variable $X_{PU,k}$ and is realized as (Rodriguez-Parera et al., 2008) follows:

$$\bar{P}_{d_{avg}} = E(X_{1PU,k}, X_{2PU,k} \dots X_{N_r PU,k}(P_d|X_{1PU,k}, X_{2PU,k} \dots X_{N_r PU,k})) \tag{11}$$

$$= \int_{X_{1PU,k}=0}^{\infty} \dots \int_{X_{NrPU,k}=0}^{\infty} P_d|X_{PU,k} p_{X_{PU,k}}(X_{PU,k}) dX_{PU,k} \tag{12}$$

$$= \int_{X_{1PU,k}=0}^{\infty} \dots \int_{X_{N_r PU,k}=0}^{\infty} Q\left(\frac{\gamma - (\sigma^2_{W,k} + \sigma^2_{S_{SI},k} + X_{PU,k})}{\sqrt{\frac{2(\sigma^4_{W,k}+\sigma^4_{S_{SI},k}+X^2_{PU,k})}{N_r N_t N_f}}}\right) p_{X_{PU,k}}(X_{PU,k}) dX_{PU,k}, \tag{13}$$

Here, $p_{X_{PU,k}}(X_{PU,k})$ is the PDF of $X_{PU,k}$. $p_{X_{PU,k}}(X_{PU,k})$ depends on the power profile of channel and total number of channel taps, L. Now, considering unequal power for each channel tap of multipath fading channel model, the $p_{X_{PU,k}}(X_{PU,k})$ is expressed as (Rodriguez-Parera et al., 2008):

$$p_{X_{PU,k}}(X_{PU,k}) = \sum_{l=0}^{L-1} \frac{\alpha_l}{\sigma^2_h(l)} \exp\left(\frac{-X_{PU,k}}{\sigma^2_h(l)}\right), \tag{14}$$

Here $\alpha_l = \prod_{i=0, i\neq l}^{L-1} \frac{1}{1-\sigma^2_h(i)/\sigma^2_h(l)}$. Next, a new digital domain SI cancelation using the LS technique followed by wavelet denoising is employed to suppress the RSI received under H_1.

3.2. Digital Domain RSI Cancelation Using Noise Robust Wavelet Decomposition-Based LS Technique

This section is divided into two subsections. In the first subsection, using conventional LS technique, the SI channel estimate is first obtained considering desired signal transmitter off and further obtained considering desired signal as noise. Here, block-type pilot arrangement for PU signal is considered, where all subcarrier of an OFDM symbol for PU signal are assigned to pilots (Lee et al., 2009). Since SI signal is the signal imposed by the transmit antenna on the receive antenna within the same transceiver, it is assumed to be known to the SU (Afifi & Krunz, 2015). In the next subsection, noise robust SI channel estimation is performed by employing wavelet denoising on the initial SI channel estimates obtained using conventional LS technique under the aforementioned schemes. The block diagram representing the proposed algorithm employing wavelet denoising is shown in Figure 4.

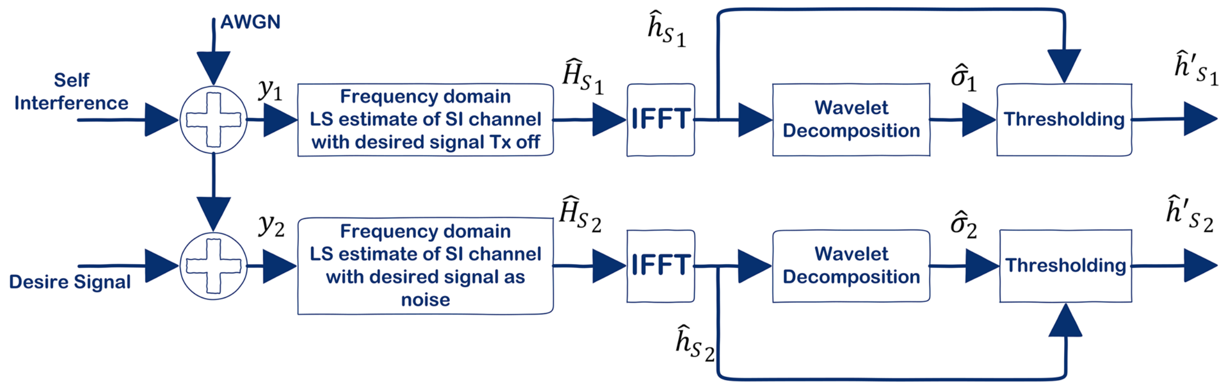

Figure 4. Block diagram of the proposed algorithm using wavelet decomposition.

3.2.1. Conventional LS Estimation

In the first scheme, where it is considered that the desired signal transmitter is off, the signal received at FD radio receiver is expressed as follows:

$$y_1(n) = s(n) * h_{s1}(n) + w_1(n), \tag{15}$$

Here h_{s1} is single tap Rayleigh fading SI channel coefficient of SI signal under first scheme. After implementing FFT operation on the received signal represented by (15), the signal in frequency domain is represented as follows:

$$Y_1(f) = S(f)H_{s1}(f) + W_1(f). \tag{16}$$

Next, the SI channel estimate is obtained using LS method in frequency domain as (Cheng & Dahlhaus, 2002; Lee et al., 2009) follows:

$$\hat{H}_{s1}(f) = \frac{Y_1(f)}{S(f)} = H_{s1}(f) + W_1'(f), \tag{17}$$

where $W_1'(f)$ represents a noise component existing at the estimated SI channel coefficient. The time domain SI channel estimate is now obtained by taking inverse FFT (IFFT) of the frequency domain estimated SI channel coefficient expressed in 17.

$$\hat{h}_{s1} = IFFT(\hat{H}_{s1}(f)) \tag{18}$$

Further, in the second scheme, considering desired signal transmitter on, the received signal at FD radio receiver is expressed as follows:

$$y_2(n) = x(n) * h(n) + s(n) * h_{s2}(n) + w_2(n), \tag{19}$$

Here, $h_{s2}(n)$ is the single tap Rayleigh fading channel coefficient of SI signal under second scheme and $h(n)$ is the discrete time Rayleigh channel coefficients of the desired signal $x(n)$ given as follows:

$$h(n) = \sum_{l=0}^{L-1} \alpha_l \delta(n-l), \tag{20}$$

where α_l represents the attenuation associated with lth path and l represents the different path delay index. L is the total number of channel taps. Considering the desired signal as noise, the received signal could be expressed as follows:

$$y_2(n) = s(n) * h_{s2}(n) + w_2'(n). \tag{21}$$

Again applying LS in frequency domain, the SI channel estimate is obtained as (Cheng & Dahlhaus, 2002; Lee et al., 2009) follows:

$$\hat{H}_{s2}(f) = \frac{Y_2(f)}{S(f)} = H_{s2}(f) + W_2'(f), \tag{22}$$

where $W_2'(f)$ represents a noise component existing at the estimated SI channel coefficient. Now by applying IFFT operation on the obtained frequency domain SI channel estimate, the time domain SI channel estimate is expressed as follows:

$$\hat{h}_{s2} = IFFT(\hat{H}_{s2}(f)) \tag{23}$$

3.2.2. Noise Robust Channel Estimation-Based on Wavelet Decomposition

The channel estimation is the basic requirement for coherent detection in OFDM systems, but the LS algorithm does not care about noise in obtaining its solution, so it is subjected to noise. To overcome this, wavelet denoising is performed in time domain over the LS estimate of the SI channel obtained under the two different schemes discussed in the previous subsection. In wavelet decomposition scheme, signals are divided into approximation and detail coefficients. Smoothing filters like moving averaging filters are used to obtain approximation coefficients, and similarly, detail coefficients are obtained using high-pass filters. The smoothing filter impulse response $h'(n)$ and high-pass filter impulse response $g'(n)$ used for the Haar wavelet are represented as (Lee et al., 2009) follows:

$$\begin{aligned} h'(n) &= \frac{1}{2}(\delta[n] + \delta[n+1]) \\ g'(n) &= \frac{1}{2}(\delta[n] - \delta[n+1]) \end{aligned} \tag{24}$$

where δ is the Kronecker delta function and is expressed as follows:

$$\delta[n] = \begin{cases} 1, & n = 0 \\ 0, & n \neq 0 \end{cases} \tag{25}$$

The frequency response of the impulse responses $h'(n)$ and $g'(n)$ of the smoothing and high-pass filters, respectively, can be obtained as follows:

$$H'(e^{jw}) = e^{\left(\frac{jw}{2}\right)} cos\left(\frac{\hat{w}}{2}\right) \tag{26}$$

Here, $\hat{w}$ is defined as the radian frequency.

The standard deviation of the detail coefficients corresponding to noise added to the signal could be obtained (Rao & Bopardidar, 1998) as follows:

$$\hat{\sigma}_i = \frac{median|D_i|}{0.6745}, \tag{27}$$

where $i = 1, 2$ corresponds to the schemes considering desired signal transmitter off and desired signal as noise, respectively. D_i represents the detail coefficients obtained employing discrete wavelet transform (DWT) on the SI channel coefficient estimate obtained using LS estimation and the obtained $\hat{\sigma}_i$ is used as a threshold value. To employ wavelet denoising, thresholding operation is performed on the SI channel estimates obtained in both the schemes considering desired signal transmitter off and desired signal as noise, respectively, to obtain noise robust SI channel coefficient estimates. Initially, wavelet denoising is employed on the SI channel estimate obtained using LS technique considering the first scheme and the corresponding noise robust SI channel estimates are expressed as follows:

$$\hat{h}'_{s1} = \begin{cases} \hat{h}_{s1}, & \hat{h}_{s1} \geq \hat{\sigma}_1, \\ 0, & \hat{h}_{s1} < \hat{\sigma}_1, \end{cases} \tag{28}$$

Here, $\hat{\sigma}_1$ represents the standard deviation of the detail coefficient corresponding to first SI cancelation scheme considering desired signal transmitter off. Further, for performing RSI cancelation, first, SI signal estimate is obtained as $\hat{s}_1 = s(n) * \hat{h'}_{s1}$ and it is subtracted from the total received signal, $y(n)$ at FD radio receiver which is expressed as follows:

$$y_1'(n) = y(n) - \hat{s}_1. \tag{29}$$

Algorithm 1 : The proposed algorithm for RSI cancellation using wavelet decomposition based LS technique.

Require: : Pilot symbols for the desired signal.

- Obtain SI channel estimate, $\hat{h}_{s1}$ and $\hat{h}_{s2}$ considering desired signal transmitter off and desired signal as noise respectively
- Employ DWT on $\hat{h}_{s1}$ and $\hat{h}_{s2}$ to obtain $\hat{\sigma_1}$ and $\hat{\sigma_2}$ respectively from detail coefficient D_i
- **if** $\hat{h}_{s1} \geq \hat{\sigma_1}$ **then**
  $\hat{h'}_{s1} = \hat{h}_{s1}$
- **else if** $\hat{h}_{s1} < \hat{\sigma_1}$ **then**
  $\hat{h'}_{s1} = 0$
- **end if**
- Obtain SI signal estimate $\hat{s}_1$
- Perform SI cancellation to obtain $y'_1 = y - \hat{s}_1$
- Similarly,
- **if** $\hat{h}_{s2} \geq \hat{\sigma_2}$ **then**
  $\hat{h'}_{s2} = \hat{h}_{s2}$
- **else if** $\hat{h}_{s2} < \hat{\sigma_2}$ **then**
  $\hat{h'}_{s2} = 0$
- **end if**
- Obtain SI signal estimate $\hat{s}_2$
- Perform SI cancellation to obtain $y'_2 = y - \hat{s}_2$

Similarly, applying thresholding operation on the SI channel estimate obtained using LS technique under the second scheme considering desired signal as noise, noise robust SI channel coefficient estimates are expressed as follows:

$$\hat{h}'_{s2} = \begin{cases} \hat{h}_{s2}, & \hat{h}_{s2} \geq \hat{\sigma}_2, \\ 0, & \hat{h}_{s2} < \hat{\sigma}_2. \end{cases} \tag{30}$$

Here, $\hat{\sigma}_2$ represents the standard deviation of the detail coefficient corresponding to SI cancelation scheme considering desired signal as noise. Again, under this scheme, SI signal is canceled by subtracting SI signal

Table 1
Simulation Parameters

Parameters	$\bar{P}_d$ versus P_{fa} for different *SNR* values	$\bar{P}_d$ versus *SNR* for different N_t and N_f values	$\bar{P}_d$ versus *SNR* for different N_r values
Number of Monte Carlo iterations	2,000	2,000	2,000
Modulation technique	QPSK OFDM	QPSK OFDM	QPSK OFDM
Number of OFDM symbols	100	100	100
Number of subbands	64	64	64
Window length in time domain, N_t	11	9, 15, 21	11
Window length in frequency domain, N_f	4	2, 4, 6	4
Number of receive antenna, N_r	4	4	2, 4, 8, 16
P_{fa}	0 to 1	0.001	0.001
SNR (dB)	−5, 0, 5	−10 to 20	−10 to 20

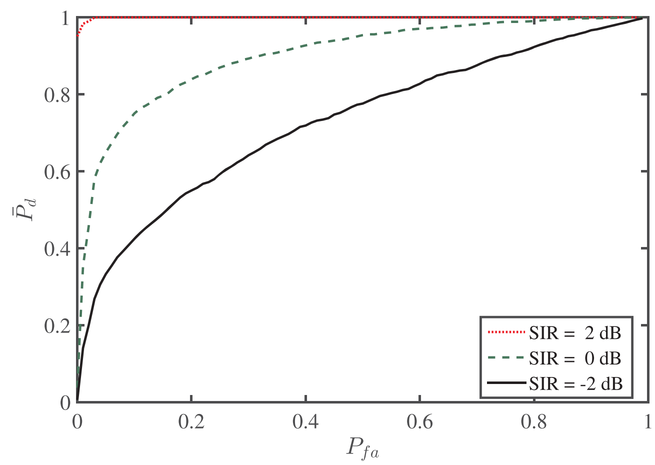

Figure 5. $\bar{P}_d$ versus P_{fa} at fixed $N_t = 11$ and $N_f = 4$ for different *SIR*.

estimate obtained as $\hat{s}_2 = s(n) * \hat{h}'_{s2}$ from the total signal received at FD radio receiver and is expressed as follows:

$$y'_1(n) = y(n) - \hat{s}_2. \tag{31}$$

The pseudocode for the proposed wavelet denoising-based LS technique under both the above discussed schemes is presented in Algorithm 1.

4. Simulation Performance

In this section, the evaluation of the proposed FFT-based energy detection technique employing two-dimensional rectangular filtering operation for multiband spectrum sensing in SIMO OFDM systems over multipath fading channel is carried out through Matlab simulations. We emphasized on receiver operating characteristic (ROC) ($\bar{P}_d$ versus P_{fa} and $\bar{P}_d$ versus *SNR*) for analyzing the detection performance of the proposed detection scheme. The simulation parameters are listed in Table 1. The various simulation parameters considered are signal-to-noise ratio (*SNR*), (signal-to-RSI ratio) *SIR*, *INR*, N_t, N_f, and the number of Monte Carlo iterations used is 2,000. System bandwidth considered is 20 MHz. The FFT size is 64, cyclic prefix length taken is 16, and number of OFDM symbols considered is 100. The conventional modulation scheme used for transmit symbols on each subcarrier is Quadrature phase shift keying (QPSK). For ease of simulation, no coding and data scrambling are used. The far end, that is, desired channels, are modeled as multipath Rayleigh fading with three channel taps each, whereas each near end SI channels are modeled as single tap fading channel. We assume that there were no frequency offset and synchronization error. To obtain the threshold value, we used D_i, which is one of the

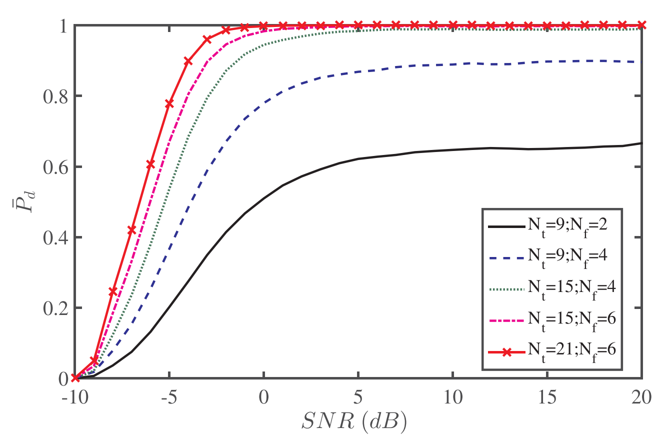

Figure 6. $\bar{P}_d$ versus *SNR* (dB) at constant $P_{fa} = 0.001$ for different N_t and N_f.

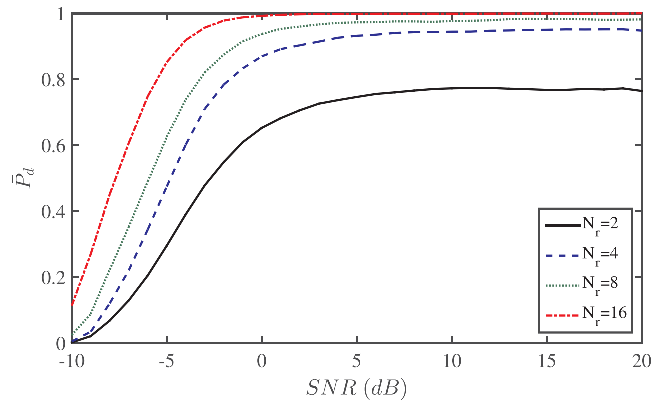

Figure 7. $\bar{P}_d$ versus *SNR* (dB) for different N_r.

well-known filters for a wavelet decomposition to estimate the channel values varying with time (Rao & Bopardidar, 1998).

The impact of *SIR* variation on detection performance is illustrated in Figure 5, which represents $\bar{P}_d$ versus P_{fa} with constant filter lengths $N_t = 11$ and $N_f = 4$ for different values of *SIR*. With decrease in *SIR*, the detection performance degrades which illustrates that the presence of high RSI power deteriorates the performance of the detector and thus to obtain a target $\bar{P}_d = 0.95$ in FDCRNs under RSI becomes a challenging task. Figure 6 represents the $\bar{P}_d$ versus *SNR* plot at constant $P_{fa} = 0.001$ for different values of N_t and N_f. This clearly shows that increase in the number of N_t and N_f improves the detection performance as large filter lengths helps in reducing the spectrum leakage influence. Similarly, $\bar{P}_d$ versus *SNR* plot for different number of receive antenna is depicted in Figure 7. The increase in the number of receive antenna improves the spatial diversity, which enhances the detection performance over multipath Rayleigh frequency selective fading channels.

Figure 8 depicts the mean square error (MSE) comparison performance of the proposed algorithm with the reported conventional techniques used for estimating SI channel in QPSK OFDM. It is clearly inferred that MSE of the proposed wavelet denoising-based LS techniques perform better than the conventional LS technique under both the schemes with desired signal transmitter off and desired signal as noise. Wavelet denoising reduces the noise effect on the SI channel estimate obtained using LS technique and thus provides better performance.

Bit error rate (BER) curves after one tap equalization followed by decoding with QPSK OFDM is shown in Figure 9. This clearly shows that the proposed scheme with wavelet denoising raises the SI channel

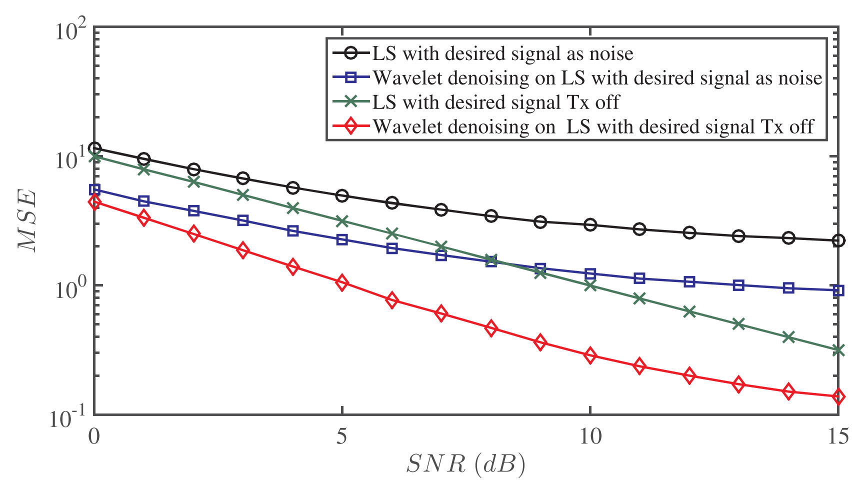

Figure 8. MSE versus SNR (dB) in QPSK OFDM FD system.

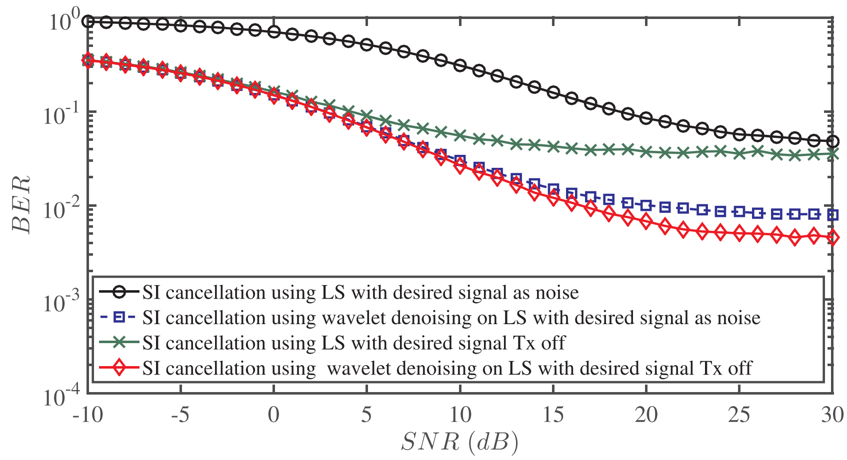

Figure 9. BER versus SNR (dB) in QPSK OFDM FD system.

estimation performance and thus reduces BER in comparison to the conventional LS technique. Finally, the detection performance employing various RSI cancelation algorithms is depicted in Figure 10. It is clearly inferred that utilizing the proposed SI cancelation algorithm using noise robust wavelet denoising-based LS technique under the scheme considering desired signal transmitter off outperforms the reported conventional LS technique under both the previously discussed schemes as well as wavelet denoising-based LS with desired signal as noise scheme.

5. Conclusion

In this work, we evaluated the performance of the FFT-based multiband spectrum sensing over multipath Rayleigh frequency selective fading channels in SIMO FDCRNs. First the analysis is carried out and the closed form expressions for $\bar{P}_d$ and P_{fa} are derived. The presence of RSI in FDCRN stimulates the detection performance degradation and to avoid RSI, a new scheme using noise robust wavelet denoising-based LS technique is employed. The simulation results show that the proposed scheme with wavelet denoising on LS considering desired signal transmitter off gives better performance in terms of MSE and BER as compared to the conventional LS techniques and LS followed by wavelet denoising approach considering desired signal as noise and it also results in improved detection performance.

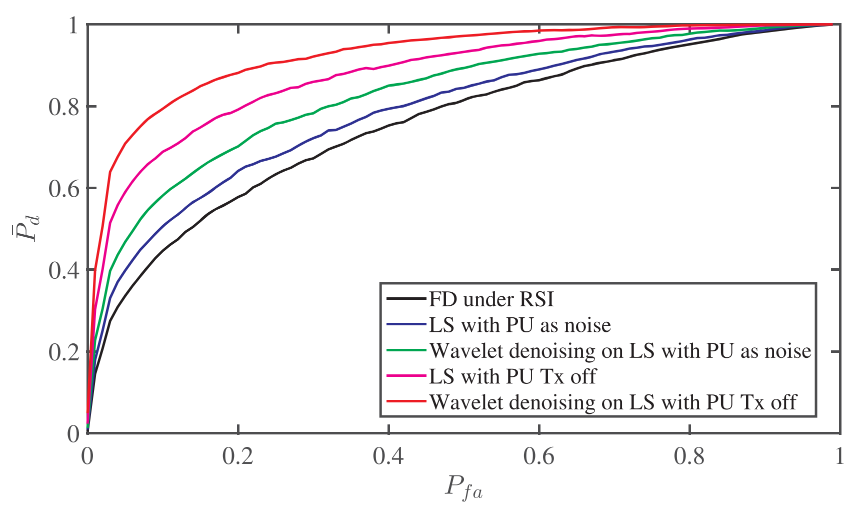

Figure 10. $\bar{P}_d$ versus P_{fa} at constant $SIR = 0$ (dB) for RSI cancelation algorithms.

Data Availability Statement

The observe data related to the this experimental work could be find at the website (https://data.mendeley.com/datasets/hwzbvmxnk6/draft?a=af2e7288-f90a-45c2-a89a-432d8fa193f9).

Acknowledgments
The author would like to acknowledge the Ministry of Electronics and Information Technology (MeitY), Government of India, for supporting the financial assistance during research work through Visvesvaraya PhD Scheme for Electronics and IT.

References

Afifi, W., & Krunz, M. (2015). Incorporating self-interference suppression for full-duplex operation in opportunistic spectrum access systems. *IEEE Transactions on Wireless Communications*, *14*(4), 2180–2191.

Arshad, K., Ali Imran, M., & Moessner, K. (2010). Collaborative spectrum sensing optimisation algorithms for cognitive radio networks. *International Journal of Digital Multimedia Broadcasting*, *2010*, 20.

Axell, E., Leus, G., & Larsson, E. G. (2012). Spectrum sensing for cognitive radio: State-of- the-art recent advances. *IEEE Signal Processing Magazine*, *29*(3), 101–116.

Badawy, A., Khattab, T., Elfouly, T., Chiasserini, C.-F., & Trinchero, D. (2016). On the performance of spectrum sensing based on GLR for full-duplex cognitive radio networks.

Bloomfield, P. (2000). *Fourier analysis of time series: An introduction*. John Wiley.

Cheng, Z., & Dahlhaus, D. (2002). Time versus frequency domain channel estimation for OFDM systems with antenna arrays. In *IEEE 6th International Conference on Signal Processing* (pp. 1340–1343). Zurich, Switzerland.

Dikmese, S., Gokceoglu, A., Valkama, M., & Renfors, M. (2013). Reduced complexity spectrum sensing based on maximum eigenvalue and energy. In *Proceeding ISWCS* (pp. 1–5). Ilmenau, Germany.

Dikmese, S., Renfors, M., & Dincer, H. (2011). FFT and filter bank based spectrum sensing for WLAN signals. In *Proc. ECCTD* (pp. 781–784). Linkoping, Sweden.

Dikmese, S., Sofotasios, P. C., Ihalainnen, T., & Renfors, M. (2015). Efficient energy detection methods for spectrum sensing under non-flat spectral characteristics. *IEEE Journal on Selected Areas in Communications*, *33*(5), 755–770.

Dikmese, S., Srinivasan, S., & Renfors, M. (2012). Spectrum sensing and spectrum utilization model for OFDM and FBMC based cognitive radios. In *Proc. SPAWC* (pp. 139–143). Cesme, Turkey.

Haykin, S. (2005). Cognitive radio: Brain-empowered wireless communications. *IEEE Journal on Selected Areas in Communications*, *23*(2), 201–220.

Hossain, E., Niyato, D., & Han, Z. (2009). *Dynamic spectrum access and management in cognitive radio networks*. UK: Cambridge University Press.

Huang, Y., & Huang, X. (2013). Detection of temporally correlated signals over multipath fading channels. *IEEE Transaction on Wireless Communication*, *12*(3), 1290–1299.

Lee, Y.-S., Shin, H.-C., & Kim, H.-N. (2009). Channel estimation based on a time-domain threshold for OFDM systems. *IEEE Transaction on Broadcasting*, *55*(3), 656–662.

Liao, Y., Wang, T., Song, L., & Jiao, B. (2014). Cooperative spectrum sensing for full-duplex cognitive radio networks. In *IEEE International Conference on Communication Systems (ICCS)* (pp. 56–60). Macau.

Masmoudi, A., & Le-Ngoc, T. (2015). Self-interference cancellation for full-duplex MIMO transceiver. In *IEEE wireless communications and networking conference (WCNC)* (pp. 141–146). New Orleans, LA, USA.

Nguyen, D., Tran, L.-N., Pirinen, P., & Latva-aho, M. (2014). On the spectral efficiency of full-duplex small cell wireless systems. *IEEE Transactions on Wireless Communications*, *13*(9), 4896–4910.

Rao, R. M., & Bopardidar, A. S. (1998). Wavelet transforms introduction to theory and applications. 24 Prime Park Way, Natick, MA 01760-1500: The MathWorks, Inc.

Report, T. (2002). *Spectrum policy task force report*. DC, USA: Federal Commun. Commission, Washington.

Riihonen, T., & Wichman, R. (2014). Energy detection in full-duplex cognitive radios under residual self-interference. In *9th International Conference on Cognitive Radio Oriented Wireless Networks and Communications (CROWNCOM)* (pp. 57–60. Oulu, Finland.

Rodriguez-Parera, S., Ramon, V., Bourdoux, A., Horlin, F., & Lauwereins, R. (2008). Spectrum sensing over SIMO multi-path fading channels based on energy detection. In *IEEE Global Telecommunications Conference (GLOBECOM)*, New Orleans, LO, USA, pp. 1–6.

Tandra, R., & Sahai, A. (2005). Fundamental limits on detection in low SNR under noise uncertainty. In *Proceeding, International Conference Wireless Network Communication Mobile Computing*, (pp. 464–469).

Tripta, Kumar, A., & Saha, S. (2017). Performance evaluation of NP and ML based spectrum sensing in FDCRNs under small scale fading scenario. In *IEEE Region 10 Conference (TENCON)* (pp. 2051–2055). Malaysia.

Vilar, G. V., Valcarce, R. L., & Sala, J. (2011). Multiantenna spectrum sensing exploiting spectral a priori information. *IEEE Transaction on Wireless Communication*, *10*(12), 4345–4355.

Wang, X. (2011). Joint sensing-channel selection and power control for cognitive radios. *IEEE Transaction on Wireless Communication*, *10*(3), 958–967.

Yucek, T., & Arslan, H. (2009). A survey of spectrum sensing algorithms for cognitive radio applications. *IEEE Communications Surveys & Tutorials*, *11*(1), 116–130.